

Weak ferromagnetism of $\text{La}_{1.99}\text{Sr}_{0.01}\text{CuO}_4$ thin films: evidence for removal of corrugation in CuO_2 plane by epitaxial strain

I. Tsukada

Central Research Institute of Electric Power Industry,
2-11-1 Iwado-kita, Komae-shi, Tokyo 201-8511, JAPAN
(Dated: March 22, 2024)

The weak ferromagnetism of $\text{La}_{1.99}\text{Sr}_{0.01}\text{CuO}_4$ epitaxial thin films is investigated using magnetoresistance measurement. While a step-like negative magnetoresistance associated with the weak ferromagnetic transition is clearly observed in the films grown on YAlO_3 (001), it is notably suppressed in the films grown on SrTiO_3 (100) and $(\text{LaAlO}_3)_{0.3}(\text{SrTa}_{0.5}\text{Ta}_{0.5}\text{O}_3)_{0.7}$ (100), and almost disappears in films grown on LaSrAlO_4 (001). The strong suppression of the step-like magnetoresistance provides evidence that the CuO_2 planes are much less corrugated in thin films grown on tetragonal substrates, particularly on LaSrAlO_4 (001), than in bulk crystals.

PACS numbers: 74.25.Fy, 74.72.Dn, 75.50.Ee, 74.78.Bz

Epitaxial growth of $\text{La}_{2-x}\text{Sr}_x\text{CuO}_4$ (LSCO) and $\text{La}_{2-x}\text{Ba}_x\text{CuO}_4$ (LBCO) superconductors has been gathering much attention since a remarkable increase in T_c was reported for films grown on LaSrAlO_4 (001).^{1,2,3} In these studies, in-plane compressive and out-of-plane tensile strains applied to the lattice were found to be favorable for the increase of T_c . As is widely known, bulk crystals of LSCO have two phases: high-temperature tetragonal (HTT, $I4mm$) and low-temperature orthorhombic (LTO, $Bmab$) phases. In the LTO phase, a staggered rotation of the CuO_6 octahedra gives rise to the characteristic corrugation in the CuO_2 plane. Considering that superconductivity occurs in this LTO-phase stable region for bulk unstrained crystals, we expect that the epitaxial strain affects the superconducting properties through a modification in the corrugated structure. However, it seems difficult to directly investigate a such microscopic structure in thin-film samples; we usually apply a neutron diffraction method to a bulk crystal for such purpose, but it may not apply to a thin-film sample because of its too small volume. Thus far, there has been no report on the true role of epitaxial strain of LSCO and LBCO thin films.

An indirect but prospective approach to the corrugation in the CuO_2 plane is to study an antiferromagnetic sample instead of a superconducting one, because the corrugation is strongly coupled to antiferromagnetism and weak ferromagnetism of LSCO. In the LTO phase, the corrugated structure of the CuO_2 plane allows Dzyaloshinskii-Moriya (DM) interactions to work between the nearest-neighbor spins on Cu^{2+} ions.⁴ The DM interactions consequently induce cooperative spin canting, giving rise to a weak ferromagnetic (WF) moment perpendicular to the CuO_2 plane, which alternately changes its direction along the c axis. Since the coupling of the WF moments on adjacent layers is rather weak, one can drive a WF transition by applying magnetic field along the c axis; above the critical field, the WF moments point in the same direction at every CuO_2 plane. Thio et al. have reported that the out-of-plane resistance shows a steep decrease at the critical field,⁴

indicating a strong coupling of electronic transport and magnetic ordering. Recently, Ando et al. have discovered that the in-plane magnetoresistance also exhibits a characteristic steep decrease across the WF transition.⁵ The in-plane magnetoresistance, therefore, can be a sensitive probe of the weak ferromagnetism that is strongly coupled with the corrugated structure of the CuO_2 plane. In this paper, we report the in-plane magnetoresistance for the antiferromagnetic (AF) $\text{La}_{1.99}\text{Sr}_{0.01}\text{CuO}_4$ thin films epitaxially grown on four different substrates, and discuss how the corrugation of the CuO_2 plane is modified by the epitaxial strain.

$\text{La}_{1.99}\text{Sr}_{0.01}\text{CuO}_4$ thin films were prepared by pulsed-laser deposition (KrF excimer, $\lambda = 248$ nm). Substrate temperature was kept at 800 °C during the deposition in an atmosphere of 30 mTorr oxygen. This growth condition is the same as that used for a previous report.⁶ Under this growth condition we can grow superconducting LSCO thin films with very low residual resistivity implying few crystallographic imperfections. The laser repetition rate was set at the lowest value ($f = 1$ Hz) to properly apply strain to the films. A polycrystalline sintered target of $\text{La}_{1.99}\text{Sr}_{0.01}\text{CuO}_4$ was prepared by a solid-state reaction method. At this Sr concentration, we expect that the AF long-range order appears at $T = 200$ K in a bulk crystal.⁷ The actual chemical composition of the grown film became slightly La-rich ($\text{LaSrCu} = 2.28:0.01:1.00$), but this deviation does not significantly affect the antiferromagnetism of the sample. We used four substrates: orthorhombic YAlO_3 (001) has a rectangular surface symmetry, while tetragonal LaSrAlO_4 (001), cubic $(\text{LaAlO}_3)_{0.3}(\text{SrTa}_{0.5}\text{Ta}_{0.5}\text{O}_3)_{0.7}$ (100), and cubic SrTiO_3 (100) have a square surface symmetry. Hereafter, these substrates are referred to as YAP (Yttrium Aluminum Perovskite), LSAO, LSAT, and STO, respectively. To avoid confusion, we follow the axis notation of the LTO structure of LSCO. Film thickness was set at approximately $t = 1800$ Å. After patterning the films for four-terminal measurements, they were carefully annealed at 600 °C in helium to remove extra oxygen following the procedure for lightly doped bulk crystals.⁷ Since

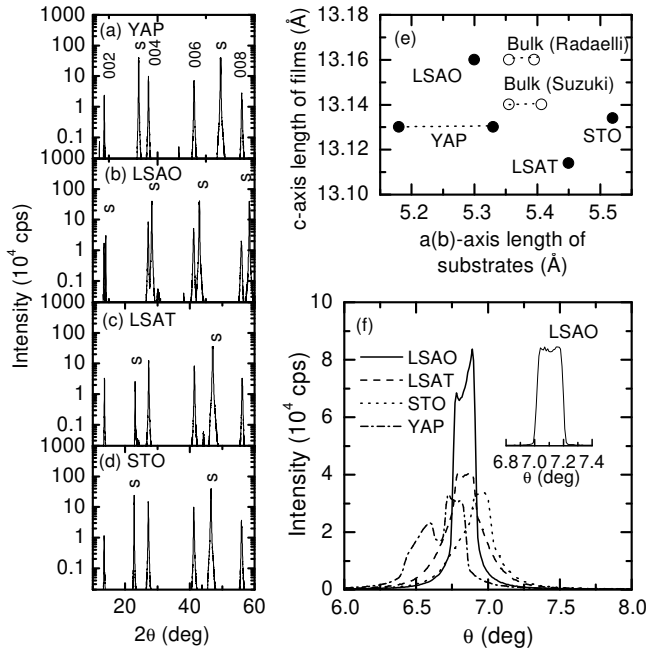


FIG. 1: (a)–(d) X-ray diffraction of the films taken by ω -2 θ goniometer. Reflections from the substrates are indicated by s. (e) Relationship between the lattice parameters of substrates and the c-axis lengths of the films. The data for bulk samples of La_2CuO_4 are taken from Refs. 9 and 10. (f) The Rocking curve of the 002 reflection. Inset shows that of LSAO substrate.

the extra oxygen can easily induce superconductivity, as discussed by Sato et al.¹ and Bozovic et al.,⁸ this post-annealing in helium is crucial for the present experiments. The in-plane resistivity was measured under the magnetic field up to 10 T by the Physical Properties Measurement System (PPMS, Quantum Design).

The x-ray diffraction shows that all the films are highly c-axis oriented as shown in Figs. 1(a)–1(d). The c-axis length estimated from all of the observed 00l (l: even) reflections is plotted as a function of the a(b)-axis length of substrates in Fig. 1(e) with the data of ceramic samples of La_2CuO_4 .^{9,10} Although the c-axis length does not show monotonic behavior at first glance, this variation is consistent with the results reported by Sato et al. for $\text{La}_{1.85}\text{Sr}_{0.15}\text{CuO}_4$ films,¹ i.e., a significant change in the c-axis length is observed only in the films with sufficiently small lattice mismatch. The marked expansion or compression of the c-axis is observed for the film grown on LSAO or LSAT. Their in-plane lattice parameters are very close to those of LSCO , which results a remarkable expansion or compression of the c-axis length. In contrast, the films grown on YAP and STO, where the lattice mismatch are much larger, do not feel the strain fully, and consequently, the c-axis length approaches a certain value that is determined only by thermodynamics. We actually observed that the c-axis lengths of these films are almost equal.

In order to see more detail, we compared the rocking

curve around the 002 reflection as shown in Fig. 1(f). The 002 reflection is the lowest-index diffraction, and considered to be the most sensitive to wide-area crystallographic quality. We see that the peak height of the film on LSAO is twice as high as that of the others, which indicates the better orientation than the others. The more important feature is, however, a shape of the peak; The peak width is the narrowest for the film on LSAO. The splitting at the peak top is due to the finite mosaicity of the LSAO substrate (see the inset), and thus, the peak width of each domain is considered to be much narrower than the width shown in Fig. 1(f). Another important feature is that this peak does not have a broad tail, which is only the case of the film on LSAO. The absence of the tail indicates that the epitaxial strain is applied entirely through the film. The contrasting behavior is observed in the films grown on LSAT and STO, where the broad tail is observed in their rocking curves. The peak structures of these films look like a superposition of a narrow intense and a broad less-intense peaks. The presence of the narrow intense peak indicates that a part of the film is well strained like the film on LSAO. However, the accompanying broad peaks suggests that the lattice relaxation occurs in another part of the films. In general, when lattice relaxation proceeds according to the film growth, the film begins to be divided into do-

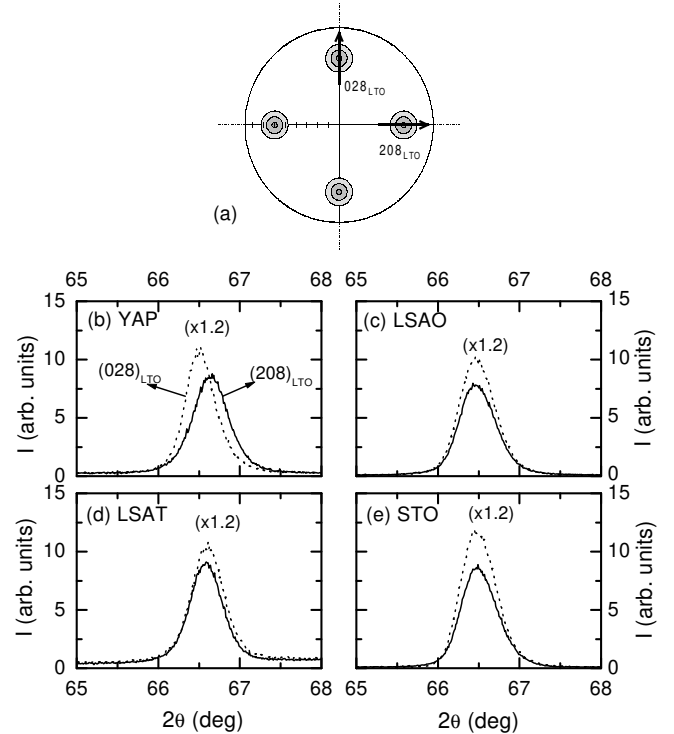


FIG. 2: (a) Schematic of 208 and 028 reflections in the pole-figure configuration. The scan directions of the peaks in (b)–(e) are indicated by arrows. (b)–(e) 208 (solid line) and 028 (dotted line) reflections of the films grown on YAP (001), LSAO (001), LSAT (100), and STO (100). The intensity of the 028 reflection is multiplied by 1.2.

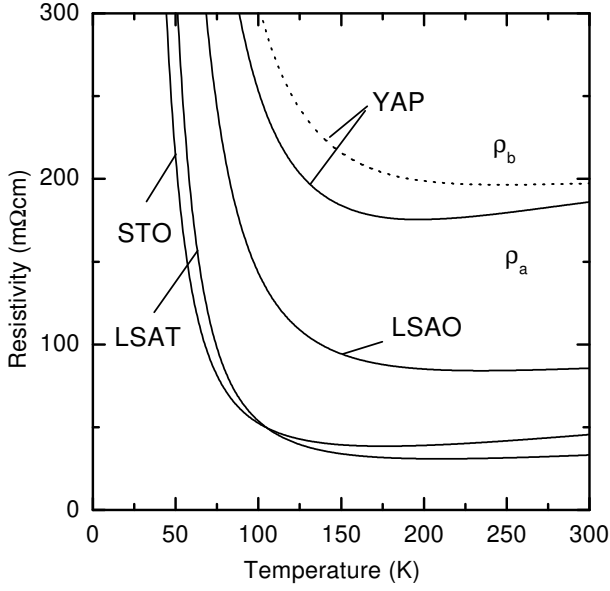


FIG. 3: Temperature dependence of the in-plane resistivity of the films. For the film grown on YAP, the resistivity is anisotropic along two orthogonal directions (solid and dotted lines), while such an anisotropy is absent in the other films.

mains with slightly different orientation when the film can no longer hold the strain. Thus, the rocking curves of these films show that the films grown on LSAT and STO may consist of lower fully-strained layers and upper less-strained (relaxed) layers. The rocking curve of the film grown on YAP looks much more complicated. However, if you look at the each peak, you can see that the peak width is comparable to the others. From this rocking curve, we expect that the lattice relaxation begins almost at the initial stage of the film growth, and thus, cracks also start to grow from the film-to-substrate interface. As will be shown later, we observe the highest resistivity in the film grown on YAP, which is consistent with this expectation.

Next, we confirmed the in-plane crystallographic symmetry. For this purpose, we used a pole-figure goniometer to scan both the 208 and 028 reflections. Figures 2(b)–2(e) show the single scans of the 208 and 028 reflections. The scan direction is indicated by an arrow in Fig. 2(a). For the film grown on YAP, the 208 and 028 reflections appear at different angles indicating the orthorhombic symmetry, and the in-plane orientation is determined as YAP [100] k LSCO [100], which may allow us to expect that the corrugation survives in the CuO_2 plane. On the other hand, the two reflections appear at the same angle for the films grown on LSAO, LSAT, and STO. However, these results do not immediately mean that these films are really tetragonal. For example, $\text{Bi}_2\text{Sr}_2\text{Ca}_{n-1}\text{Cu}_n\text{O}_{2n+4}$ is orthorhombic and does not become tetragonal even when grown on STO (100), but it exhibits a twin structure composed of orthorhombic domains.¹¹ Thus, we cannot judge whether the corru-

gation is actually removed from these three films as this stage, and therefore, the magnetoresistance measurement becomes important.

The in-plane resistivity of all films exhibit an insulating behavior upon approaching $T = 0$ K, as shown in Fig. 3. In contrast to the resistivity data reported for superconducting samples,^{1,2,3} the films grown under the compressive strain (YAP and LSAO) show a higher resistivity than those grown under the tensile strain (LSAT and STO). The film grown on YAP is orthorhombic, as was shown before, and has resistivity anisotropy along the a and b axes; ρ_a is always lower than ρ_b for this film, and the temperature where the resistivity shows a minimum value is also lower for ρ_a than for ρ_b . Such different temperature dependences are qualitatively consistent with those for bulk crystals with $x = 0.02$,¹² which supports our identification of the a - and b -axis directions. The other three films show almost no in-plane anisotropy.

After characterizing the films by x-ray diffraction and resistivity measurements, we measured the in-plane magnetoresistance. Figures 4(a) and 4(b) show the magnetoresistance measured at $T = 40$ K and its first derivative, respectively, in which we can easily see a marked difference between the film grown on YAP and those grown on the others. The film grown on YAP exhibits a clear step-like magnetoresistance, like bulk crystals do.⁵ As shown in Fig. 4(c), $R(H) = R(0)$ at $T = 200$ K is almost field-independent up to $H = 10$ T, while below $T = 150$ K, $R(H) = R(0)$ shows an apparent decrease above approximately $H = 2$ T; a steep decrease begins at $H = 2$ T and almost ends at $H = 6$ T. For convenience, we will define the WF transition field as the field where the first derivative shows a minimum. According to this definition, $H_{WF} = 4$ T is obtained for this film as indicated by an arrow in Fig. 4(b). From the magnetoresistance data, we can roughly estimate the Néel temperature (T_N) for this film by plotting the temperature dependence of $R(H) = R(0)$ at several fields (Fig. 5). $R(H) = R(0)$ is almost zero at $H < H_{WF}$ (1 and 2 T) through the temperature range below 300 K, while the deviation to negative values becomes apparent below $T = 200$ K when the field is higher than H_{WF} (6 and 10 T). As a result, the AF long-range order is considered to set in at approximately $T = 200$ K. This assignment is consistent with T_N reported for bulk crystals.⁷

The other three films grown on tetragonal surfaces show contrasting behavior. The step-like magnetoresistance behavior is strongly suppressed in comparison with the films grown on YAP. At $T = 40$ K and $H = 10$ T, $R(H) = R(0)$ reaches only -1.1% (LSAO), -0.9% (LSAT), and -1.4% (STO), which are far smaller than that observed for the film grown on YAP. Nevertheless, one can find traces of the WF transition in the films grown on LSAT and STO. Figure 4(b) shows that the WF transition still occurs at $H_{WF} = 2.5$ T for these two films, even though the critical field is lower than that for the film on YAP. In these films, we may expect that T_N shifts to lower temperatures. As shown in Fig. 4(e), the mag-

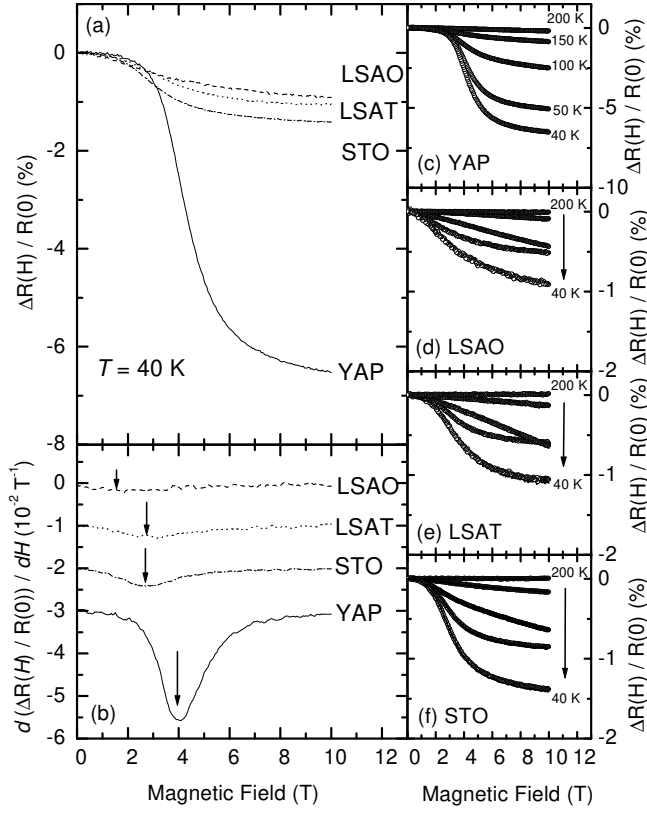


FIG. 4: (a) In-plane magnetoresistance of $\text{La}_{1.99}\text{Sr}_{0.01}\text{CuO}_4$ thin films measured at $T = 40$ K. The large step-like negative magnetoresistance associated with the WF transition, which is significant in the film grown on YAP, almost disappears in the films grown on LSAO, LSAT, and STO. (b) The first derivative of the magnetoresistance shown in (a). (c)-(f) The temperature variations of the in-plane magnetoresistance for each film.

netoresistance of the film on LSAT maintains a convex upward- field dependence even at $T = 100$ K and a trace of the step-like behavior appears only below $T = 50$ K, which suggests that the T_N of this film is found between 50 and 100 K.

The weak ferromagnetism is more strongly suppressed in the film grown on LSAO, and the first derivative of the magnetoresistance becomes almost field-independent. We can no longer obtain clear H_{WF} from Fig. 4(b). If one carefully analyzes Fig. 4(b), H_{WF} is still discernible around $H = 1.5$ T. However, this value is even lower than the H_{WF} 's of the films grown on LSAT and STO, and we conclude that the weak ferromagnetism is most strongly suppressed in the film grown on LSAO.

One may wonder if the result obtained above is strongly dependent on film thickness, because the lattice strain applied from substrate may be relaxed by increasing the film thickness in general, which will result a recovery of step-like magnetoresistance. Since the film grown on LSAT indicates slight but finite corrugations in the CuO_2 plane as is implied from Fig. 3, LSAT is considered to be the most appropriate substrate to study

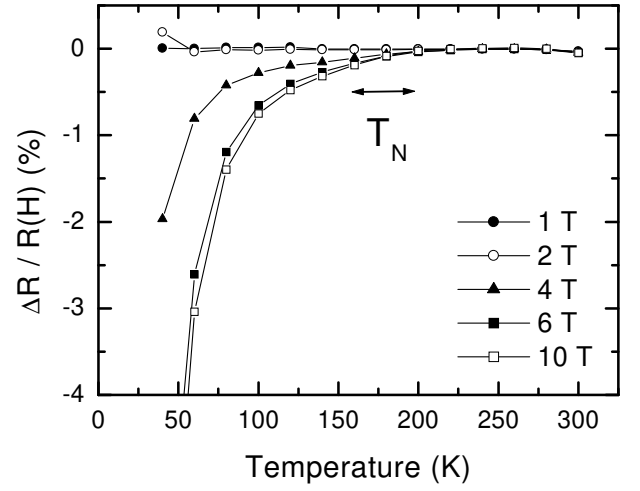


FIG. 5: Temperature dependence of the magnetoresistance for $\text{La}_{1.99}\text{Sr}_{0.01}\text{CuO}_4$ film grown on YAP (001) measured at $H = 1, 2, 4, 6,$ and 10 T.

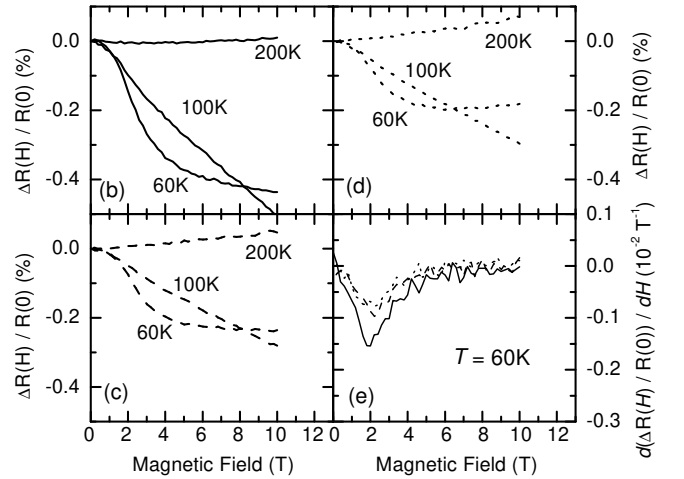
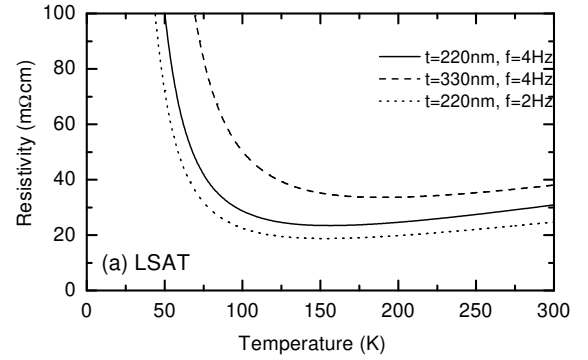


FIG. 6: (a) Temperature dependence of the in-plane resistivity of $\text{La}_{1.99}\text{Sr}_{0.01}\text{CuO}_4$ thin film on LSAT (100) prepared under the conditions different from those shown in Figs. 2 and 3. (b) The magnetoresistance of the film ($t = 2200$ Å) prepared at $f = 4$ Hz. (c) The magnetoresistance of the film ($t = 3300$ Å) prepared at $f = 4$ Hz. (d) The magnetoresistance of the film ($t = 2200$ Å) prepared at $f = 2$ Hz. (e) The first derivative of the magnetoresistance at $T = 60$ K shown in (b)-(d).

the thickness dependence. Figure 6 shows the resistivity and magnetoresistance of the films grown on LSAT (100) prepared under the condition different from that for the film shown in Fig. 4: $t = 2200 \text{ \AA}$ at $f = 4 \text{ Hz}$, $t = 3300 \text{ \AA}$ at $f = 4 \text{ Hz}$, and $t = 2200 \text{ \AA}$ at $f = 2 \text{ Hz}$. Although the magnitude of the resistivity is not completely identical, its temperature dependence is similar to one another and that for typical insulating LSCO with $x = 0.01$ as shown in Fig. 6(a).⁵ Figures 6(b) – 6(d) show the magnetoresistance measured at $T = 200, 100$, and 60 K . It is easily seen that all the films exhibit almost the same behavior as that in Fig. 4(e). At $T = 200 \text{ K}$, the magnetoresistance is slightly positive and almost featureless. When temperature is decreased down to 100 K , the negative magnetoresistance becomes apparent, but step-like behavior is still absent. After the temperature is decreased to 60 K , the step-like behavior shows up. What we should emphasize is that the overall magnetoresistance behavior is qualitatively the same among Figs. 4(e), 6(b)–6(d). The magnitude of magnetoresistance at $H = 10 \text{ T}$ is less than 0.5% at $T = 60 \text{ K}$, again suggesting the corrugation of the CuO_2 plane remains but its tilting is strongly suppressed. The first derivative of the magnetoresistance traces almost the identical line (Fig. 6(e)), which suggests the weak-ferromagnetic transition occurs at the same field regardless of the film thickness. As a result, we may safely conclude that the general behavior of the magnetoresistance shown in Fig. 4 is not so strongly dependent on the film thickness and/or the growth condition.

We are now ready to discuss the microscopic structure of the CuO_2 plane. As has been reported for $\text{La}_2\text{CuO}_{4+x}$ (Ref. 4) and $\text{La}_{1.99}\text{Sr}_{0.01}\text{CuO}_4$ (Ref. 5) single crystals, the magnetic field applied parallel to the c axis induces a WF transition at the critical field $H_{WF} \approx 4\text{--}5 \text{ T}$, which is accompanied by a large step-like negative magnetoresistance. Whatever the origin of this peculiar magnetoresistance is,^{5,13} the WF transition is the most clear evidence of a finite spin canting out of the CuO_2 plane that is inherent in the corrugated structure of CuO_2 planes characteristic of the LTO phase. The present results indicate that the film grown on YAP actually has a corrugation in the CuO_2 plane similar to that in bulk crystals. The experimentally determined $H_{WF} (\approx 4 \text{ T})$ implies that the film grown on YAP is almost identical to bulk crystals, because single crystals show almost the same transition field.⁵ However, it should be noted that the transition width across H_{WF} is broader in this film than in reported crystals.^{4,5} This suggests a spatial inhomogeneity of the transition field due to a finite lattice mismatch between the crystal and the substrate.

The magnetoresistance of the films grown on LSAT and STO is interesting. As shown in Fig. 1(e), the c -axis lengths of these films are shorter than that of the bulk crystals. This implies that the tensile strain is actually applied to the films, and thus we may expect the symmetry of CuO_2 planes to become tetragonal following the substrate symmetry. On the other hand, as can be

seen in Figs. 4(a) and 4(b), a weakened but finite step-like magnetoresistance remains, indicating that the corrugation in the CuO_2 plane survives. The most probable explanation is that these films are separated in two parts: lower fully-strained layer and upper relaxed layer, and the corrugation structure remaining in the relaxed layer is responsible for the step-like magnetoresistance. If lattice relaxation proceeds, the crystal will approach its original form with finite corrugation in the CuO_2 plane. However, there is no sign of bulk orthorhombicity in these films as is demonstrated by Figs. 2(d) and 2(e). In order to explain these results self-consistently, we expect the film to have a microscopic twin structure: the films are separated into domains that are still orthorhombic but their orthorhombicity is not as large as in the films grown on YAP. In this case, the corrugation in the CuO_2 plane is reasonably suppressed leading to the reduction in the WF moment. Certainly, the magnitude of the WF moment cannot be evaluated directly from the magnetoresistance. However, if the reduction in the WF moment really takes place, a substantial suppression of the effective interplane coupling can be deduced from the experimentally observed reduction of H_{WF} , because the product of H_{WF} and the magnitude of the WF moment is roughly proportional to the effective inter-plane coupling. Such suppression of the interplane coupling is consistent with the scenario that the symmetry of CuO_2 planes becomes less orthorhombic.

Our results also show an advantage of LSAO over other substrates. The weak ferromagnetism is more strongly suppressed in the film grown on LSAO than in films grown on LSAT or STO. This is probably because that the lattice mismatch of LSCO to LSAO is smaller than those to STO and LSAT.¹⁴ We emphasize that not only the tensile strain but also the compressive strain is helpful in removing the corrugation from the CuO_2 plane. This cannot be simply understood because the presence of corrugation implies that the CuO_2 plane has already been compressed by a rather small La_2O_3 blocking layer. With respect to this point, our results strongly indicate that the substrate symmetry is also essential for the removal of corrugation, and that the tetragonal substrate works well for these particular LSCO thin films.

Finally, let us briefly discuss the AF long-range order in these films, because not only H_{WF} but also T_N seems to be affected by the epitaxial strain. Figures 4(c)–4(f) show the magnetoresistance measured at $T = 100 \text{ K}$. In the film grown on YAP and STO, we can find weak ferromagnetism at this temperature, indicating that T_N of these films is higher than 100 K . On the other hand, the magnetoresistance data for the films grown on LSAO and LSAT show no such features, suggesting that the system is still in the paramagnetic phase, and the latter two films probably have lower T_N 's than the former ones or the bulk crystals. We consider that the reduction in T_N is also caused by the tetragonal symmetry that the substrate introduces to the film. If CuO_2 planes are truly tetragonal and, at, the inter-plane exchange in-

interactions between the nearest-neighbor Cu ions on the adjacent layers are strongly frustrated. Consequently, a strong reduction in the effective interplane interactions is expected, which should suppress the formation of the magnetic long-range order. Thus, the reduction in T_N together with H_{WF} also confirms that the films become less orthorhombic.

To summarize, we have found that the in-plane magnetoresistance of antiferromagnetic LSCO thin films is strongly dependent on the substrate material. The difference in the magnetoresistance behavior is attributed

to the change in the corrugation structure of the CuO_2 plane. Within our experiments, the flattest CuO_2 plane is obtained in films grown on LaSrAlO_4 (001) substrates. It is suggested that not only the lattice parameters of the substrate but also its symmetry plays a significant role in removing the corrugations. We expect that a similar epitaxial strain works in superconducting LSCO thin films accounting for the observed T_c enhancement.

The author thanks A. N. Lavrov, Seiki Komiyama, and Yoichi Ando for stimulating discussions and also for a critical reading of the manuscript.

Electronic address: ichiro@criepidenken.or.jp

- ¹ H. Sato and M. Naito, *Physica C* 274, 221 (1997); H. Sato, A. Tsukada, M. Naito, and A. Matsuda, *Phys. Rev. B* 61, 12447 (2000).
- ² H. Sato, A. Tsukada, M. Naito, and A. Matsuda, *Phys. Rev. B* 62, R799 (2000).
- ³ J.-P. Locquet, J. Perret, J. Fompeyrine, E. Machler, J. W. Seo, and G. Van Tendeloo, *Nature (London)* 394, 453 (1998).
- ⁴ T. Thio, T. R. Thurston, N. W. Preyer, P. J. Picone, M. A. Kastner, H. P. Jenssen, D. R. Gabbe, C. Y. Chen, R. J. Birgeneau, and A. Aharony, *Phys. Rev. B* 38, 905 (1988).
- ⁵ Y. Ando, A. N. Lavrov, and S. Komiyama, *Phys. Rev. Lett.* 90, 247003 (2003).
- ⁶ A. N. Lavrov, I. Tsukada, and Y. Ando, *Phys. Rev. B* 68, 094506 (2003).
- ⁷ A. N. Lavrov, Y. Ando, S. Komiyama, and I. Tsukada, *Phys. Rev. Lett.* 87, 017007 (2001).
- ⁸ I. Bozovic, G. Logvenov, I. Belca, B. Narimbetov, and I. Sveklo, *Phys. Rev. Lett.* 89, 107001 (2002).

- ⁹ P. G. Radaelli, D. G. Hinks, A. W. Mitchell, B. A. Hunter, J. L. Wagner, B. Dabrowski, K. G. Vandervoort, H. K. Viswanathan, and J. D. Jorgensen, *Phys. Rev. B* 49, 4163 (1994).
- ¹⁰ T. Suzuki and T. Fujita, *Physica C* 159, 111 (1989).
- ¹¹ J. N. Eckstein, I. Bozovic, K. E. von Dönnenberg, D. G. Schlom, J. S. Harris, Jr., and S. M. Baumann, *Appl. Phys. Lett.* 57, 931 (1990).
- ¹² Y. Ando, K. Segawa, S. Komiyama, and A. N. Lavrov, *Phys. Rev. Lett.* 88, 137005 (2002).
- ¹³ L. Shekhtman, I. Ya. Korenblit, and A. Aharony, *Phys. Rev. B* 49, 7080 (1994).
- ¹⁴ We should calculate the misfit both along the *a* and *b* axis for LTO/LSCO. By using the lattice parameters of bulk samples (Ref. [10]), the misfit is 0.85% (*k*_a) and 1.60% (*k*_b) to LSAO, -2.10% (*k*_a) and -1.37% (*k*_b) to LSAT, and -2.99% (*k*_a) and -2.26% (*k*_b) to STO. The smallest misfit is achieved to LSAO both along *a* and along *b*.